https://doi.org/10.70750/GEP.2025.3-4.19

A TDOA MÓDSZER HATÉKONYSÁGÁNAK VIZSGÁLATA L-ALAKÚ ACÉLLEMEZEN

EFFICIENCY TEST OF THE TDOA METHOD ON L-SHAPE METAL PLATE

Kriston J. Balázs[*], *Dr. Jálics Károly*[**]

ABSTRACT

In this study, the application of the Time Difference of Arrival (TDoA) method was investigated to locate impulse excitations in steel components. The research employs a hierarchical modeling approach, beginning with simple rectangular steel plates, advancing to bent L-shaped plates, and ultimately targeting realistic car chassis elements. This article highlights how structural features influence wave propagation and localization accuracy. The results demonstrate that TDoA can reliably identify impulse locations in simple structures, highlighting its potential as a robust tool for diagnostics in automotive engineering. The study provides a foundational framework for extending TDoA-based diagnostics from laboratory-scale experiments to full-scale vehicle applications.

1. INTRODUCTION

Traditional vibration-diagnostic approaches often rely on frequency-domain analyses, which have only limited ability to detect the location of the malfunction and uncover the root cause e.g in a motor vehicle. Introducing TDoA into vibration diagnostics offers a promising new approach to identifying and localizing impulse excitations in complex mechanical systems. The principle of TDoA is straightforward: when an impulse signal is generated, it propagates through the structure and is detected at spatially distributed sensors with small differences in arrival time. By analyzing these delays, the source position of the event can be estimated with high accuracy. To explore the feasibility of this method, simplified mechanical models are first developed, enabling systematic testing of applicability of TDoA to vibration signals in controlled settings. The goal is to achieve reliable impulse detection and localization in real-world vehicle structures.

During the adaptation of the source localization procedure to vibration signals, the steps of the process that are necessary for successful pulse source determination were developed:

1. **Capture raw t_i time signals**
   Min. 3 sensors must be used; impulse should be located within the convex geometric shape formed by the accelerometers.
2. **Under sampling**
   Eliminates disturbing frequency components.
3. **Signal prewhitening**
   Signal preconditioning before cross-correlation. Eliminates auto-correlation between time series, therefore it improves the accuracy of time delay estimation.
4. **Optional: autocorrelation (ACF)**
   Check the effectiveness of prewhitening. ACF should be 0.
5. **Cross correlation (CCF)**
   Estimate the time delay of arrival between the reference and other sensors.
6. **Determine wave speed**
   Calculate sound wave speed for Nyquist-frequency, considering the dispersion of bending waves in plates.
7. **Calculate coordinates (SX-method)**
   The mathematical background for source coordinate calculation, based on the least squares method. SX = Spherical Intersection.
8. **Result evaluation and visualization**
   The visualization of the quadratic equation to be solved is a parabola, the roots of the function contain the source coordinates.

2. WAVE PROPAGATION IN COMPLEX STRUCTURES

In plate-like components - such as the vehicle body elements - the propagation velocity is strongly frequency dependent. The frequency dependence of the velocity of sound is called dispersion. The phase velocity of waves in plates can be calculated as follows [1]:

$$c_B = \sqrt{\omega} \cdot \sqrt[4]{\frac{B}{h}}, \tag{1}$$

where

$$B = \frac{h^3}{12} \cdot \frac{E}{1-\nu^2} \tag{2}$$

is the bending stiffness. Performing the calculations with the parameters $h = 1/1.56$ mm; $E = 210 \cdot 10^3$ MPa; $\nu = 0{,}3$; $\rho = 7850\ \mathrm{kg/m^3}$ the frequency-dependent

* *PhD student, University of Miskolc, Institute of Machine and Product Design*
** *Head of Institute, University of Miskolc, Institute of Machine and Product Design*

curve for the propagation velocity shown in Figure 1 is obtained.

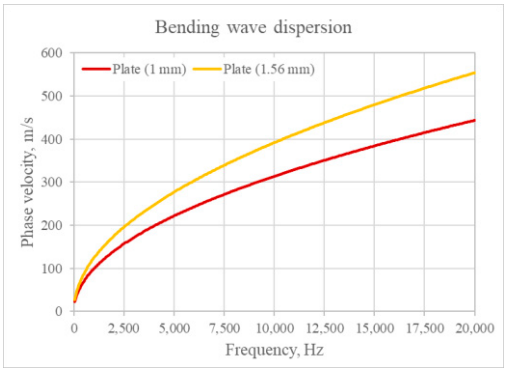

Figure 1. Frequency-dependent sound wave propagation

The response signals are elongated along the time axis, since vibrations with different frequencies arrive at the sensors at different times due to their different propagation speeds.

3. TDoA MEASUREMENT ON RECTANGULAR PLATE

Accordingly, we consider a simplified (2D) model to explore the influencing factors and possibilities of the procedure. In this stage of the tests artificial excitation was used and the impact was applied by an impulse hammer on the plate in Figure 2.

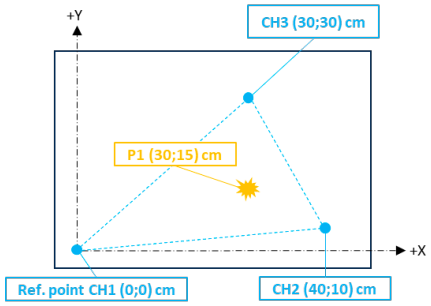

Figure 2. Coordinates of measurement and excitation points on rectangular steel plate

One of the accelerometers (CH1) was defined as a reference point with coordinates (0;0) cm. The other sensor positions and the excitation point were randomly determined. The dimensions of the rectangular plate were: 50 x 46 x 0.156 cm (length x width x thickness). The plate was placed on sponges fitted to its four corners during the test. So, the structure at point P1 was hit and the impulse responses with the vibration acceleration sensors (CH1…CH3) were recorded.

Applying cross-correlation to the pre-whitened signal, we obtain the time difference of the arrival of sound waves at the sensors. The maximum coefficient of the cross-correlation function gives the time value of the delay (Figure 3). Lag is the time interval between events recorded in a regular manner and with a constant period. In our case, a period can be understood as the reciprocal of the sampling frequency, which is $1{,}2 \cdot 10^{-4}$ sec after 8192 Hz under sampling.

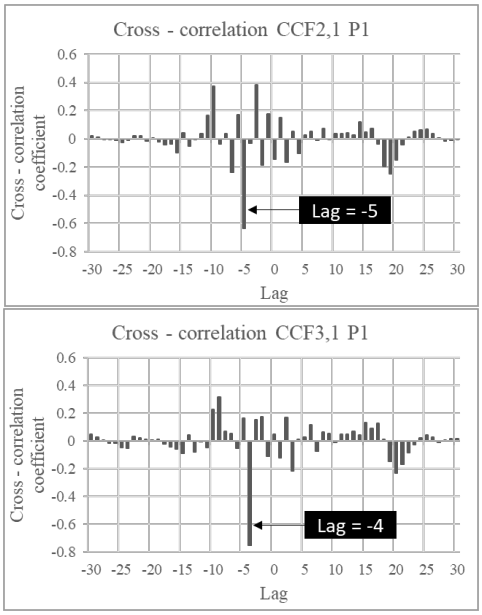

Figure 3. CCF formed from the measurement points (CH1 ...CH3) during the excitation of the P1 point

The time difference between CH1 reference point and CH2 measurement point is $6{,}103 \cdot 10^{-4}$ sec, while between CH1 reference point and CH3 measurement point is $4{,}882 \cdot 10^{-4}$ sec. Assuming homogeneous wave propagation, phase velocity $c_B = 354$ m/s. Utilizing the measured data as input for the SX method (programmed in GNU Octave) the following coordinates were calculated for the P1 excitation point: $X = 29{,}51$ cm and $Y = 14{,}38$ cm.

The coordinate of the impulse applied at location P1 (X30; Y15) can be determined with a deviation of 0.5 cm in the X-direction and 0.62 cm in the Y-direction using the established source localization routine. Therefore, the TDoA method in a simplified model, with appropriate preprocessing of the vibration signal can determine the origin of an artificial, single-source pulse-like excitation in the assigned coordinate system, within an acceptable error margin.

4. MODIFICATION OF THE ALGORITHM FOR SHAPED STRUCTURES

To continue the investigations, an L-shaped plate was fabricated, bent at 90 degrees with a 60–40% ratio. The bending radius is 2 mm (R). The geometrical dimensions of the plate are: 60 cm in width (W), 100 cm in height (L), and 1 mm in thickness (h). The plate is made of steel. The objective of this study is to evaluate the applicability of the TDoA method in the case of a three-dimensional structure, thereby providing a gradual step toward accurately describing the actual geometry and vibrational behavior of the vehicle body structure.

At the bending point of the plate — provided that the bending radius is sufficiently small compared to the plate thickness — the transverse bending wave is transformed into a longitudinal wave. A guideline in the literature states that for at least $R/h \lesssim 3$, the plate can be considered as strongly curved [2][3][4].

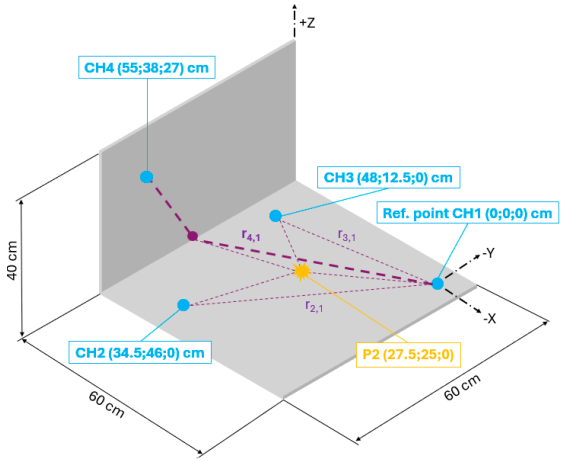

Figure 4. Coordinates of measurement and excitation points on bent steel plate

The current implementation of the TDoA algorithm cannot handle the transformation of the vibration wave at the bending point; even though such conditions are often encountered in engineering practice. On the horizontal plate segment, the signal propagates over a distance $r_{2,1}$ within a time interval $d^t_{2,1}$with a velocity $c^t_{2,1}$ characteristic of a transverse wave, whereas on the other segment it propagates over a distance $r_{4,1}$within a time interval $d^t_{4,1} + d^l_{4,1}$with velocities $c^t_{4,1} + c^l_{4,1}$, corresponding to both transverse and longitudinal wave components. Thus, during propagation toward sensor CH4, the vibration wave initially travels transversely, and after the bending point, it continues as a longitudinal wave. The impact point (P2) is located near the center of the horizontal plate. As the structure is three-dimensional, the measurement configuration consists of four sensors positioned in a Cartesian coordinate system.

The distances between sensors CH2 and CH3 and the reference sensor (CH1) are defined as:

$$r_{2,1} = c^t_{2,1} \cdot d^t_{2,1} \quad (3)$$
$$r_{3,1} = c^t_{3,1} \cdot d^t_{3,1} \quad (4)$$

The distance between the CH4 sensor located on the vertical plate and the reference sensor (CH1) is:

$$r_{4,1} = c^t_{4,1} \cdot d^t_{4,1} + c^l_{4,1} \cdot d^l_{4,1} \quad (5)$$

It can be observed from eq. (5) that the total time delay $d_{4,1}$, determined from the measurement, consists of two unknown components corresponding to different propagation velocities. For better interpretability of analysis, the plate is unfolded.

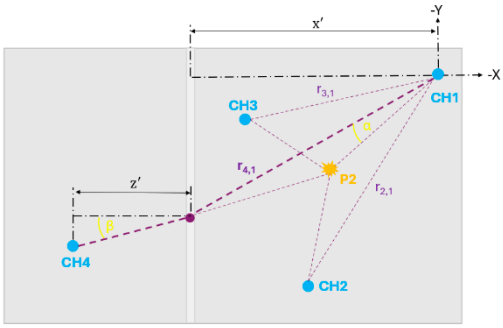

Figure 5. Unfolded view of the bent plate

The propagation angles (α, β) are illustrated approximately only for visualization purposes. From the model, the distances $r_{(i,1)}$ can also be expressed in terms of geometry.

$$c^t_{4,1} \cdot d^t_{4,1} = \frac{x'}{\cos\alpha} \quad (6)$$
$$c^l_{4,1} \cdot d^l_{4,1} = \frac{z'}{\cos\beta} \quad (7)$$

Next, the relationship between longitudinal and transverse wave propagation is examined. The velocity of the longitudinal wave is given by:

$$\left(c^l_{i,1}\right)^2 = \frac{E(1-\nu)}{\rho(1+\nu)(1-2\nu)} \quad (8)$$

The velocity of the transverse wave is:

$$\left(c^t_{i,1}\right)^2 = \frac{G}{\rho} = \frac{E}{2\rho(1+\nu)} \quad (9)$$

By substituting the typical Poisson's ratio of 0.3 for steel into the two equations, the following is obtained:

$$c^l_{i,1} = 1{,}87 \cdot c^t_{i,1} \quad (10)$$

This relationship establishes a relationship between the propagation velocities of the two types of waves. It is important to note that, due to the dispersion of the transverse wave, the formula is valid for a specific, constant frequency. The longitudinal wave velocity depends only on the material properties and geometry. By substituting this relationship into Eq. (5), $r_{4,1}$ can be expressed as:

$$r_{4,1} = c^t_{4,1}(d^l_{4,1} + 1{,}87 d^t_{4,1}) \quad (11)$$
$$d_{4,1} = d^l_{4,1} + d^t_{4,1} \quad (12)$$

The system of Eqs. (11) and (12) contain two unknowns ($d^l_{4,1}$ and $d^t_{4,1}$). To fully resolve this, it is necessary to introduce a ratio as a boundary condition:

$$\lambda = \frac{d_{4,1}^{t}}{d_{4,1}^{l}} \tag{15}$$

After substitution and simplification, the final form is:

$$r_{4,1} = c_{4,1}^{t} \cdot \frac{1 + 1{,}87\lambda}{1 + \lambda} \cdot d_{4,1} \tag{16}$$

With the utilization of Eg. (6) and (7) λ can be expressed:

$$\lambda = \frac{1{,}87 \cdot x' \cdot \cos\beta}{z' \cdot \cos\alpha} = \frac{d_{4,1}^{t}}{d_{4,1}^{l}} \tag{17}$$

The unknown constant λ is obtained if:

$$x' \cdot \cos\beta = z' \cdot \cos\alpha \tag{18}$$

This represents a geometric condition, implying that the transverse and longitudinal waves must propagate over equal path lengths. Considering Eq. (10) and using Eq. (18) along with the fact that sound propagates at a constant speed — the ratio of times, i.e., the boundary condition parameter, is:

$$\lambda = \frac{d_{4,1}^{t}}{d_{4,1}^{l}} = 1{,}87 \tag{19}$$

Therefore,

$$r_{4,1} = 1{,}56 \cdot \left(c_{4,1}^{t} \cdot d_{4,1}\right) \tag{20}$$

This relationship holds when the CH4 sensor and the CH1 reference point are symmetrically positioned with respect to the longitudinal x-axis of the plate, and the two sensors are equidistant from the bending point. Any X-direction error due to asymmetry can be estimated from the known geometry and propagation speed.

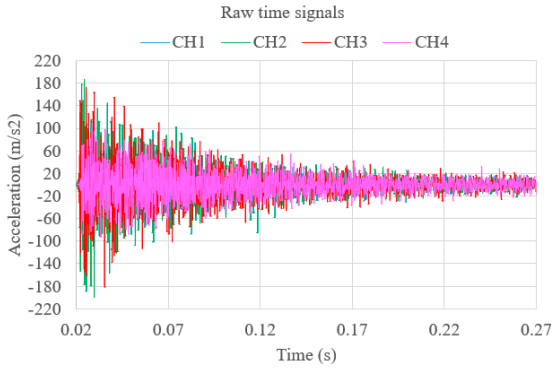

Figure 6. Raw time signals of acc. sensors

However, since the wave refraction point is not known with 100% certainty, the estimation of Y-direction error is uncertain and may distort the calculated coordinates if the boundary condition is not satisfied. From the measurement setup it is clearly visible that the boundary condition is not fulfilled. Figure 5 shows the vibration signals in the time domain received by individual acceleration sensors. The waveform corresponds to a characteristic transient excitation generated by the impulse in P2 position. The expected theoretical error in the coordinates, when the time signal is under sampled at 4096 Hz in the X-direction, is approximately 8 cm (ΔX). By performing the source localization routine on the raw time signals we obtain the time delay of arrivals. The time difference between CH1 reference point and CH2 measurement point is $9{,}765 \cdot 10^{-4}$ sec, between CH1 reference point and CH3 measurement point is $2{,}444 \cdot 10^{-4}$ sec. The time delay between CH1 and CH4, considering the theoretical position error, is $5{,}051 \cdot 10^{-3}$ sec. The phase velocity for sampled frequencies is $c_B = 143$ m/s.

Application of the SX method yields the following coordinates: $X - \Delta X = 30{,}12$ cm and $Y = 22{,}61$ cm. So, the P2 impulse point can be estimated with a rough deviation of 2,5 cm. This result considers the violation of the boundary condition and the natural inaccuracy of the method, furthermore the disturbing effect of wave propagation in the bended section.

5. SUMMARY

In the first stage, tests on a rectangular steel plate demonstrated that, after appropriate signal preprocessing the localization algorithm can accurately estimate the source location of an impulse excitation under simple geometric conditions. In the second stage, the analysis of the L-shaped plate was simplified to a two-dimensional problem, where wave mode conversion occurs at the bending point. A geometric model was developed to describe this transformation, introducing a boundary condition ($\lambda = 1.87$) representing the ratio of the propagation times of the two wave types. Achieved accuracy with the modified algorithm is 2,5 cm on a bent plate with continuous cross section.

5. REFERENCES

[1] Frank Fahy: Foundations of Engineering Acoustics 2001, Section 10.6, Academic Press, London, 2000 ISBN: 9780122476655

[2] Ka Lok Jimmy Fong: A study of curvature effects on guided elastic waves, PhD thesis, Imperial College London 2005, p. 83

[3] De Luca, A.; Perfetto, D.; Polverino, A.; Aversano, A.; Caputo, F. Finite Element Modeling Approaches, Experimentally Assessed, for the Simulation of Guided Wave Propagation in Composites. *Sustainability* 2022, *14*, 6924. ISSN: 2071-1050 https://doi.org/10.3390/su14116924

[4] Guilherme André Santana et al.: Finite element evaluation of the effects of curvature in Lamb waves for composites structural health monitoring, Latin American Journal of Solids and Structures, 2018, 15(10), e127 ISSN online version: 1679-7825 https://doi.org/10.1590/1679-78255193